Journal of Medicinal Chemistry

Article

pubs.acs.org/jmc

P2-Substituted *N*-Acylprolylpyrrolidine Inhibitors of Prolyl Oligopeptidase: Biochemical Evaluation, Binding Mode Determination, and Assessment in a Cellular Model of Synucleinopathy

Pieter Van der Veken,*[,†] Vilmos Fülöp,[‡] Dean Rea,[‡] Melanie Gerard,[§] Roos Van Elzen,[∥] Jurgen Joossens,[†] Jonathan D. Cheng,[⊥] Veerle Baekelandt,[#] Ingrid De Meester,[∥] Anne-Marie Lambeir,[∥] and Koen Augustyns[†]

[†]Laboratory of Medicinal Chemistry, Department of Pharmaceutical Sciences, University of Antwerp, Universiteitsplein 1, B-2610 Antwerp, Belgium

[‡]School of Life Sciences, University of Warwick, Coventry CV4 7AL, U.K.

[§]Laboratory of Biochemistry, Interdisciplinary Research Facility Life Sciences, KU Leuven KULAK, B-8500 Kortrijk, Belgium

[∥]Laboratory of Medical Biochemistry, Department of Pharmaceutical Sciences, University of Antwerp, Universiteitsplein 1, B-2610 Antwerp, Belgium

[⊥]Fox Chase Cancer Center, 333 Cottman Avenue, Philadelphia, Pennsylvania 19111, United States

[#]Laboratory for Neurobiology and Gene Therapy, KU Leuven, Kapucijnenvoer 33, B-3000 Leuven, Belgium

Supporting Information

ABSTRACT: We have investigated the effect of regiospecifically introducing substituents in the P2 part of the typical dipeptide derived basic structure of PREP inhibitors. This hitherto unexplored modification type can be used to improve target affinity, selectivity, and physicochemical parameters in drug discovery programs focusing on PREP inhibitors. Biochemical evaluation of the produced inhibitors identified several substituent types that significantly increase target affinity, thereby reducing the need for an electrophilic "warhead" functionality. Pronounced PREP specificity within the group of Clan SC proteases was generally observed. Omission of the P1 electrophilic function did not affect the overall binding mode of three representative compounds, as studied by X-ray crystallography, while the P2 substituents were demonstrated to be accommodated in a cavity of PREP that, to date, has not been probed by inhibitors. Finally, we report on results of selected inhibitors in a SH-SY5Y cellular model of synucleinopathy and demonstrate a significant antiaggregation effect on α-synuclein.

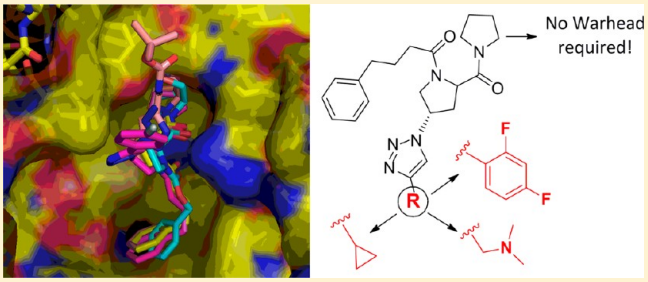

INTRODUCTION

Prolyl oligopeptidase (EC 3.4.21.29, PREP, PO, POP) was first discovered as an oxytocin degrading, post-proline cleaving peptidase.[1] Apart from oxytocin, numerous other peptides have since been reported as substrates for PREP in vitro and in vivo.[2,3] Since PREP activity in the brain is high and several neuropeptides are cleaved by the enzyme, a physiological role in neuropeptide processing and turnover is widely predicted. Several PREP inhibitors developed during the 1990s were found to have a positive effect on memory, learning, and cognition in animal models of Alzheimer's disease and brain injury, and at least two of them have been tested in humans.[2,6] Nonetheless, to date, no PREP inhibitors have been approved for therapeutic use. The in vivo effect of these inhibitors was ascribed to the prolonged action of specific neuropeptides, known to be involved in memory, learning, and cognition.[7] However, not all results of these experiments have been equivocal, and so far, no clear picture has emerged that defines the enzyme's position in the known pathways of peptide processing and degradation.[8] Over the past decade, functional PREP research has broadened its scope. It now no longer exclusively focuses on the enzyme's hydrolase activity but also addresses potential intracellular actions that affect signal transduction, protein secretion, aging, neuronal development, and differentiation.[9−20] Several of these studies indicate that protein−protein interactions underlay the role of PREP in the central nervous system, and the list of proteins that have been found to interact with PREP includes the growth associated protein GAP43, β-tubulin, and α-synuclein. However, our own

Received: July 20, 2012
Published: November 2, 2012

observation that active site inhibitors of PREP can also affect these protein−protein interactions remains enigmatic and is a topic that calls for the mechanistic reinvestigation of in vivo effects reported earlier.[20] The recent resurgence in functional PREP research, resulting from these findings, has already led to the production of PREP knockout mice and a new burst in inhibitor development.[11−13]

Most reported synthetic PREP inhibitors, extensively reviewed in 2010 by Lawandi et al., possess a dipeptde or in some cases tripeptide derived structure.[21] Relevant examples are shown in Figure 1.[22] These compounds typically interact

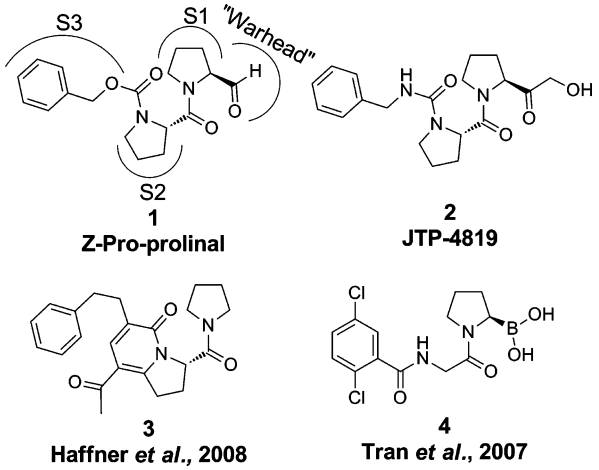

Figure 1. Relevant literature examples of PREP-inhibitors.[22a−d]

with three substrate binding sites of the enzyme: the S1 pocket which accommodates the substrate's P1-proline residue, the S2 which is less well-defined and known to accommodate several types of residues, and the S3 that is usually filled by an aliphatic spacer attached to an aromatic group. Additionally, a substantial fraction of compounds reported are characterized by the presence of a P1 "warhead": an electrophilic functional group that is capable of covalently interacting, either reversibly or irreversibly, with PREP's catalytically active serine hydroxyl group. Warhead types that have been built into PREP inhibitors include aldehyde, keto, carbonitrile, and boronate functional groups. Warhead functionalities do not necessarily limit the druglikeness of inhibitors (as demonstrated, for example, by the marketed DPP IV inhibitors vildagliptin and saxagliptin) and have the potential to significantly increase target affinity.[23] Nonetheless, the presence of these electrophiles could also be expected to have a negative influence on inhibitor stability and might perturb the selectivity profile of the inhibitors. The selectivity issue certainly deserves consideration, since a substantial number of proline-selective proteases, phylogenetically related to PREP, are present in eukaryotic genomes.[23] According to the classification of Rawlings and Barrett, these are grouped in Clan SC and include the dipeptidyl peptidases (DPPs: DPP IV, DPP II, DPP8, and DPP9) and fibroblast activation protein (FAP) that has mixed endopeptidase and dipeptidyl peptidase activity. As the DPPs use a protonated, positively charged free P2-α-amine group as an important determinant for recognition of substrates and inhibitors, PREP inhibitors (possessing a nonbasic, acylated P2-α-amine group) harbor greater undesired reactivity toward FAP than DPPs. While acylation of the P2 amine function is indeed known to generally alleviate DPP-selectivity issues, it also decreases the aqueous solubility of PREP inhibitors.

In an ongoing effort to design new generations of PREP inhibitors with improved activity, selectivity, and biopharmaceutical profile, we studied PREP−inhibitor complex crystal structures reported in the literature and present in the PDB.[24] In all of these structures, there is space to introduce substituents in the P2 position that could extend beyond the S2 binding site to probe hitherto unexplored regions of the enzyme. We decided to test this approach using the prolylpyrrolidine scaffold, since this structure forms the basis of several potent PREP and DPP IV inhibitors that have demonstrated in vivo activity in relevant animal models.[4−8,25] We predicted that grafting substituents onto the P2-prolyl residue of this scaffold could be used to (1) increase the enzyme−inhibitor affinity and thus reduce the need for the potentially problematic "warhead" functionality, (2) divert compounds away from the generic dipeptide-derived structure of most existing PREP inhibitors, hopefully leading to improved selectivity over identified and as yet unidentified potential off-targets of PREP inhibitors, and (3) introduce functionalities that modify physicochemical compound parameters, such as aqueous solubility. In this paper we describe the synthesis, potency, and specificity of the series of P2-substituted PREP inhibitors that were designed to meet these goals, along with the X-ray crystal structures of PREP in complex with a selection of these compounds. In addition, screening results are reported for selected compounds in a cellular model of synucleinopathy.

DESIGN AND SYNTHESIS OF INHIBITORS

On the basis of the existing PDB structures of PREP−inhibitor complexes and subsequent docking experiments, we identified the 4-position of the P2-prolyl residue as the preferential position to introduce substituents (Figure 2). Synthetically, we

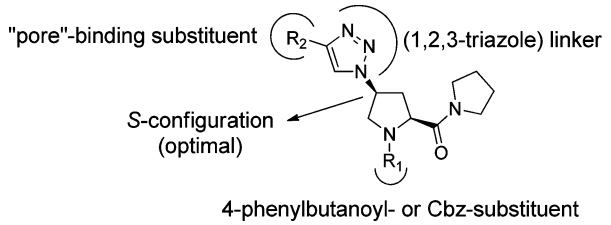

Figure 2. Generic overview of target compound structures.

opted to exploit the 1,3-dipolar Huisgen addition ("click" chemistry) for substituent introduction while also taking advantage of the metabolically stable triazole ring for linking the substituent to the inhibitor core. From design studies, a relative cis-positioning of the substituent and the proline carboxylate residue (2*S*,4*S* configuration) was predicted to be optimal. This configuration in our docking model also allowed hydrogen bond formation between the enzyme's backbone and the N3 of the triazole ring. Nonetheless, we also decided to synthesize a limited number of the trans analogues (possessing the 2*S*,4*R* configuration) to validate initial observations. For the *N*-acyl substituent of the P2-prolyl residue, either a benzyloxycarbonyl ("Cbz" or "Z") or a 4-phenylbutanoyl residue was selected. Although probably suboptimal, their ease of introduction and commercial availability were considered as prime factors at this stage of research. Finally,

dx.doi.org/10.1021/jm301060g | J. Med. Chem. 2012, 55, 9856−9867

as the P1 residue, a pyrrolidine ring not equipped with a warhead function was chosen.

Synthesis of target compounds started with the single (2*S*,4*S*) and (2*S*,4*R*) diastereomers of *N*-Boc-4-azidoproline **5a** and **5b** using a published procedure.[26] These were coupled to pyrrolidine using TBTU. Deprotection of the Boc group was followed by reaction with benzyloxycarbonyl chloride or 4-phenylbutanoyl chloride to afford intermediates **7a,b** and **8**. Final products **9a−v** and **10** were obtained using the Cu(I)-catalyzed variant of the 1,3-dipolar Huisgen cycloaddition between these intermediates and a selection of alkynes (Scheme 1). This reaction exclusively yielded one regioisomeric

Scheme 1. Synthesis of Target Products 9a−v and 10[a]

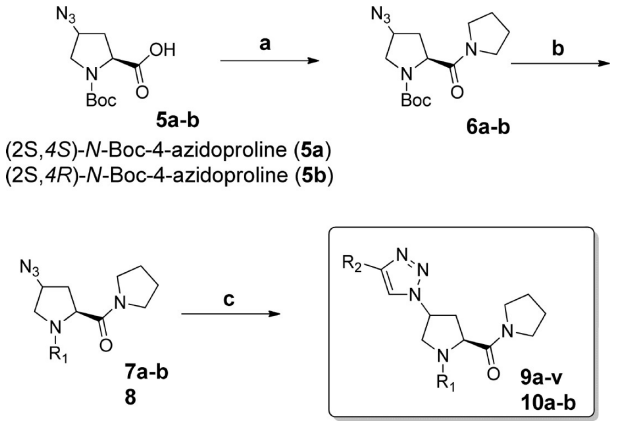

[a]Reagents and conditions: (a) pyrrolidine, TBTU, Et_3N, DMF, rt, 8 h; (b) (i) TFA, DCM, rt, 30 min; (ii) CbzCl, Et_3N, DCM, 0 °C, 2 h (R_1 = Cbz) or 4-phenylbutanoyl chloride, Et_3N, DCM, 0 °C, 2 h (R_1 = phenylbutanoyl chloride); (c) "alkyne", CuI, Et_3N (trace), MeOH, rt, 24 h. (d) If "alkyne" = trimethylsilylacetylene: KF, MeOH, rt, 48 h. If "alkyne" = *N*-Boc-propargylamine: TFA, DCM, rt, 30 min.

triazole product (the 1,4-disubstituted compound), as extensively documented by earlier literature studies of this reaction type.[27]

Although not incorporating the strategic ambitions set out in the Introduction, we decided to prepare a limited number of analogues carrying a P1-carbonitrile warhead group. We included these compounds in order to serve as additional reference compounds for validating some of the hypotheses made for target compounds **9a−v**.

The synthesis of these compounds was accomplished in a way that was similar to the strategy followed for the preparation of target compounds **9a−v**, but this time only analogues containing the (2*S*,4*S*) isomer of *N*-Boc-4-azidoproline (**5a**), expected to yield active molecules, were used. To this end, the latter was first coupled to prolinamide hydrochloride. Then acid deprotection of the Boc group was followed by introduction of a 4-phenylbutanoyl (R_1) substituent to yield compound **12**. Dehydration of the primary amide group delivered **13**, containing the carbonitrile warhead group. Since this compound already contains all necessary determinants for PREP binding, it was also evaluated as an inhibitor of the enzyme. Finally, for putting in place the triazole ring of target compound **14** (Scheme 2), the same experimental procedure was used as for the corresponding P1-pyrrolidine analogues. Under these conditions, no products of the potentially interfering, tetrazine forming [3 + 2]-cycloaddition of the

Scheme 2. Synthesis of Target Products Carrying a P1-Carbonitrile Warhead[a]

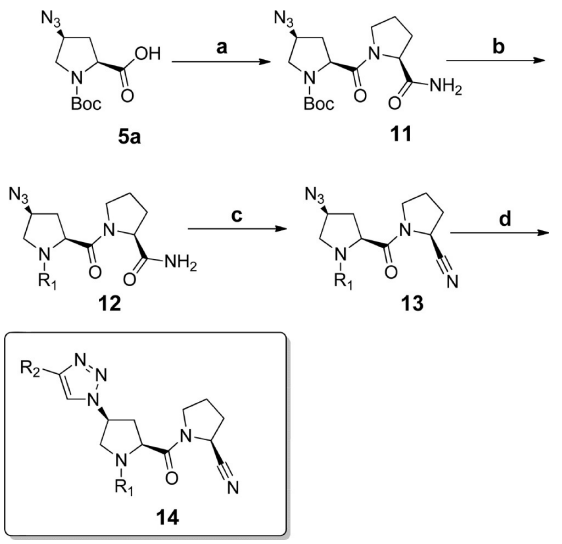

[a]Reagents and conditions: (a) prolinamide hydrochloride, TBTU, Et_3N, DMF, rt, 8 h; (b) (i) TFA, DCM, rt, quant; (ii) CbzCl, Et_3N, DCM, 0 °C (R_1 = Z) or phenylbutanoyl chloride, Et_3N, DCM, 0 °C (R_1 = phenylbutanoyl chloride); (c) trifluoroacetic anhydride, pyridine, DCM, 0 °C, 1 h; (d) *N*-Boc-propargylamine, CuI, Et_3N (trace), MeOH, rt, 24 h.

alkyne and carbonitrile function were observed in the reaction mixture.

RESULTS AND DISCUSSION

All synthesized molecules were evaluated as inhibitors of PREP, FAP, and the dipeptidyl peptidases DPP IV, DPPII, and DPP9. Although not reported, assay results for DPP8 can be expected to be comparable to data obtained in experiments with DPP9, taking into account the high degree of homology between these enzymes.[28] The prolylpyrrolidine-based PREP inhibitor **15**, reported earlier by Yoshimoto et al., and its 4-phenylbutanoyl-containing analogue **16** (SUAM-1221), taken from Atack et al., were chosen as appropriate reference compounds.[29] These molecules have the same backbones that are present in the target compounds, but they lack the substituent at the 4-position of the P2-proline residue. Hence, they can directly serve to evaluate the effect and impact of this substitution type. The IC_{50} values for PREP inhibition of the reference compounds obtained under our assay conditions are situated in the higher nanomolar range and are summarized in Table 1. Additionally, the (2*S*,4*S*)-4-azidoproline-containing intermediates **7a** and **7b** from Scheme 1 are present in this table. Inhibitory potency for these compounds is comparable to inhibitory potency obtained for the two reference compounds, and this already indicates that some additional space is available in the region of the PREP active center where the P2-proline residue is accommodated.

Inhibitory potential of the prolylpyrrolidine reference structure toward FAP and DPPs appears to be very limited from these data, raising expectations for obtaining at least a comparable degree of selectivity with respect to these proteins for the target compounds. Another observation that can already be made from the data in Table 1 and that proves to be valid as well for the target compounds (IC_{50} data summarized in Table 2) is that compounds with R_1= phenylbutanoyl display a

dx.doi.org/10.1021/jm301060g | J. Med. Chem. 2012, 55, 9856−9867

Table 1. Inhibitory Potential of Reference Compounds 15 and 16 and Azide-Substituted Analogues 7a,b toward PREP, FAP, DPP IV, DPPII, and DPP9

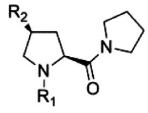

			IC_{50} (μM)				
Cmpd.	R_1	R_2	PREP	FAP	DPP IV	DPP II	DPP9
15	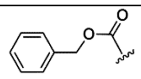	-H	0.35 ± 0.017	>>100	>>100	>>100	>100
16	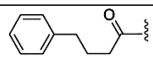	-H	0.13 ± 0.01	>>100	>>100	>>100	>100
7a	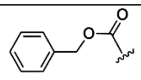	$-N_3$	0.364 ± 0.047	>>100	>>100	>>100	>100
7b	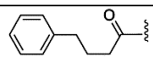	$-N_3$	0.142 ± 0.025	>>100	>>100	>100	>>100

limited but consistently higher PREP affinity than their Z-derivatized analogues. This difference explains why within the series of target compounds, a higher number of inhibitors of the former type were prepared. In cases where both the Z and phenylbutanoyl analogues of inhibitors with an identical R_2-substituent were synthesized, the corresponding assay data are presented in subsequent entries in Table 2. Compounds in Table 2 are furthermore grouped according to the structural and electronic properties of their triazole susbtituents (R_2), mainly encompassing (1) aliphatic, (2) aromatic, and (3) basic substituent types of different steric impact.

Compound **9a**, prepared from **9b** by desilylation using CsF in MeOH, represents the simplest example (R_2= H) in the series and offers the opportunity to evaluate whether the triazole ring (present in all target molecules) is indeed involved in stabilizing interactions with the enzyme as observed during docking-based design studies. Assay results for this inhibitor indicate this not to be the case. The presence of an aliphatic substituent on the triazole moiety, on the other hand, can lead to an increase in inhibitory potential with respect to the unsubstituted **9a** and the corresponding reference compounds **15** and **16** in Table 1. This is demonstrated by compound **9c**, bearing a small R_2-cyclopropyl group. The size of the substituent, however, does not seem to be of prime importance, since even the *N*-Boc-derivatized inhibitors **9e** and **9f** (used as the precursor for deprotected, basic target compound **9q**) display a potency improvement with respect to the reference compounds that is comparable to the result obtained for **9c**. For the set of inhibitors with an aromatic substituent (compounds **9g−p**), attaching an unsubstituted phenyl or pyridine ring at the triazole moiety does not lead to significant alterations in enzyme affinity with respect to the reference compounds (maximal change corresponding to a factor of 2). Halogenation of the aromatic ring (compounds **9i−m**), on the other hand, clearly has substantial impact and can lead to an increase in PREP affinity of about 1 order of magnitude. The origin of this jump in affinity is not clear and does not appear to be directly correlated to either the nature of the halogen or its position on the aromatic ring. In order to further interpret these findings, we determined the crystal structure of PREP complexed with an inhibitor from the halogenated subset. Monofluorinated compound **9i** was selected because, although not the most potent in the series, replacement of a single hydrogen atom by a very small fluorine atom already resulted in a substantial change in enzyme affinity, with little additional potency gained from additional changes. Specifically, we were wondering whether F−H hydrogen bonding with the enzyme could be involved in this (crystal structures discussed below).

Another goal of this study was to investigate whether typical solubility-enhancing (basic) groups could be added to the 4-position of the P2-proline ring while retaining or improving the inhibitory potential of the parent prolylpyrrolidine structure. Compounds **9q−v** represent the effort undertaken in this direction. In general, the assay data show that the introduction of a range of protonatable groups in this part of the inhibitors is tolerated. While most compounds possess IC_{50} values that are close to the reference compounds' (**15** and **16**), the *N*,*N*-dimethylaminomethyl-containing analogue **9r** clearly stands out in this subset, outperforming the inhibitory potential of both the corresponding reference molecule and its nonmethylated counterpart **9q** by an order of magnitude. With respect to the selectivity discussion, morpholine and piperazine-susbtituted analogues **9s−u** were found to display substantial DPP9 affinity. This is highly surprising, given the N-acylation of the α-amine function of the P2-prolyl residue in these inhibitors. A protonated amine function, known to be engaged in salt-bridging with the target protein, is present in all DPP inhibitors reported to date, either as the P2-α-amino group in peptide derived inhibitors or in a position that is topologically equivalent to the latter in non-peptide-derived compounds. Proper investigation of these findings and comparison to SAR data we have generated in the past for individual DPPs will follow in due course.[28]

As explained in the Introduction, a limited number of (2*S*,4*R*) containing analogues were also prepared in this study in order to validate initial assumptions on the expected binding mode of the target compounds (represented Table 3). Although explained more fully by the crystal structures

dx.doi.org/10.1021/jm301060g | *J. Med. Chem.* 2012, 55, 9856−9867

Table 2. Inhibitory Potential of P2-(4*S*)-Triazoloproline-Based Compounds 9a–v toward PREP, FAP, DPP IV, DPPII, and DPP9[b]

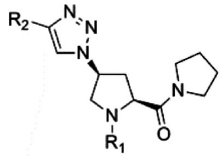

			IC_{50} (μM)				
Cmpd.	R_1	R_2	PREP	FAP	DPP IV	DPP II	DPP9
9a	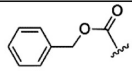	-H	1.16 ± 0.15	>>100	>100	>100	67±9
9b	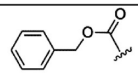		0.956 ± 0.036	>>100	>>100	>>100	>100
9c	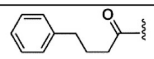		0.039 ± 0.004	>100	>100	>100	>10
9d	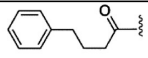		0.147 ± 0.004	>5	>>100	>>100	>100
9e	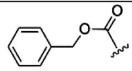	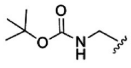	0.141 ± 0.003	>100	>>100	>>100	>10
9f	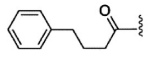	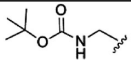	0.032 ± 0.001	>100	>100	>100	>100
9g	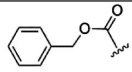		0.478 ± 0.003	n.d.[a]	>>100	>>100	>100
9h	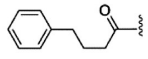		0.170 ± 0.018	n.d.	>>100	>>100	>100
9i	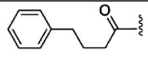	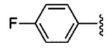	0.033 ± 0.004	n.d.	>100	>>100	>100
9j	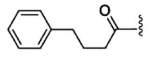	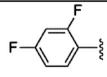	0.024 ± 0.001	>5	>100	>100	>10
9k	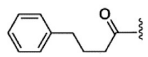	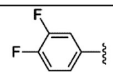	0.0172 ± 0.0007	>5	>100	>10	<100
9l	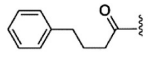		0.023 ± 0.001	>5	>100	>10	>100
9m	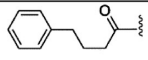	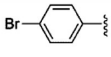	0.0140 ± 0.0007	>100	>100	>100	>10
9n	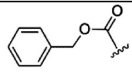		0.357 ± 0.019	>100	>>100	>>100	53 ± 5
9o	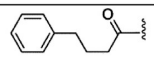		0.069 ± 0.009	>100	>>100	>>100	>100
9p	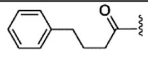	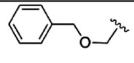	0.131 ± 0.041	n.d.	>>100	>>100	>100

dx.doi.org/10.1021/jm301060g | *J. Med. Chem.* 2012, 55, 9856–9867

Table 2. continued

			IC_{50} (μM)				
Cmpd.	R_1	R_2	PREP	FAP	DPP IV	DPP II	DPP9
9q	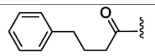		0.17 ± 0.04	>100	>100	>10	>100
9r	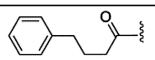		0.024 ± 0.001	n.d.	>100	>100	>10
9s	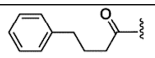	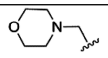	0.24 ± 0.03	>100	>50	>100	1.10 ± 0.09
9t	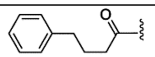	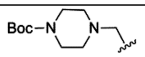	0.11 ± 0.006	>100	>100	>100	0.6 ± 0.08
9u	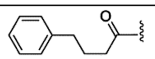	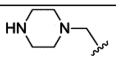	0.10 ± 0.004	>100	>100	>100	1.3 ± 0.1
9v	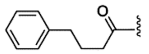		0.09 ± 0.009	n.d.	n.d.	n.d.	>10

[a]"n.d." means "not determined". [b]For compounds **9g–i** and **9p–r**, an IC_{50} for inhibition of FAP could not be determined because of compound precipitation under the FAP assay conditions. For compound **9v**, an IC_{50} for inhibition of DPP IV, DPP II, and DPP9 could not be determined because of limited compound availability.

Table 3. Inhibitory Potential of P2-(2*S*,4*R*)-Azido- and Triazoloproline-Based Compounds 8 and 10a,b toward PREP, FAP, DPP IV, DPPII, and DPP9[b]

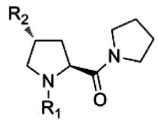

			IC_{50} (μM)				
Cmpd.	R_1	R_2	PREP	FAP	DPP IV	DPP II	DPP9
8	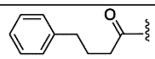	$-N_3$	0.304 ± 0.015	>>100	>>100	>100	>100
10a	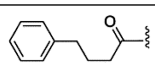	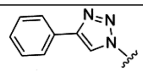	0.542 ± 0.058	n.d.[a]	>>100	>>100	>50
10b	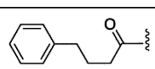	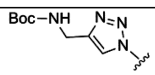	0.28 ± 0.023	>>100	>>100	>>100	>100

[a]"n.d." means "not determined". [b]Compound **10a** precipitated under the FAP-assay conditions.

(discussed below), the lower affinity of these molecules is revealed by comparing the sterically hindered compound **10b** with its (2*S*,4*S*) counterpart **9f**, in support of our original hypothesis.

Finally, although not originally part of the intention of this study, we evaluated the possibility of further increasing the affinity of P2-substituted target compounds by introduction of a carbonitrile warhead. As a reference compound, carbonitrile **17** (KYP-2047), reported earlier by Jarho et al., was synthesized and evaluated under our assay conditions (Table 4).[30]

The PREP assay data for reference compound **16** and its carbonitrile-containing analogue **17** clearly illustrate the potential of warhead introduction to increase enzyme affinity. A similar trend can be observed when comparing assay results of **7b** and that of inhibitor **13**, with the latter roughly being 2 orders of magnitude more potent. The increase in affinity is less pronounced (a factor of 3) when comparing inhibitors **9f** and **14**. This could be because accommodation of the *N*-Boc-aminomethyltriazole substituent in **14** impedes optimal orientation of the carbonitrile group for reaction with the serine hydroxyl group. To get a clearer view on this matter, compound **14** was also selected for cocrystallization with PREP.

Crystal Structures of PREP–Inhibitor Complexes. The overall binding mode of the acylated prolylpyrrolidine moiety of the three novel PREP complexes with compounds **13**, **14**,

dx.doi.org/10.1021/jm301060g | J. Med. Chem. 2012, 55, 9856–9867

Table 4. Inhibitory Potential of P1-(2*S*)-Cyanoproline-Based Compounds 13−15

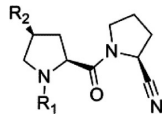

			IC_{50} (μM)				
Cmpd.	R_1	R_2	PREP	FAP	DPP IV	DPP II	DPP9
17	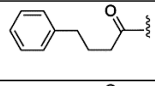	-H	0.006 ± 0.004	>10	>100	>100	>100
13	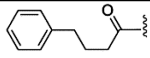	$-N_3$	0.003 ± 0.0003	>100	>>100	>>100	>100
14	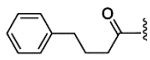	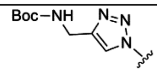	0.009 ± 0.0001	>>100	>>100	>>100	>100

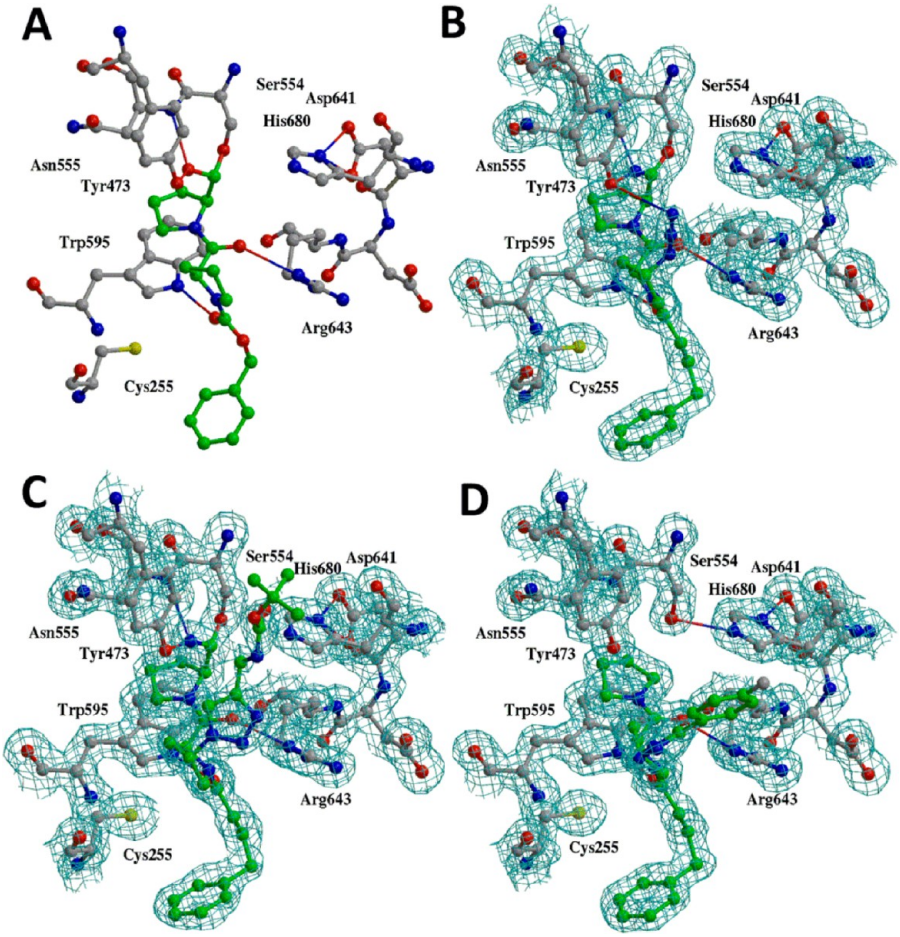

Figure 3. Crystal structures of PREP−inhibitor complexes: (A) Z-Pro-prolinal (PDB code 1qfs); (B) compound **13** (PDB code 4BCB); (C) compound **14** (PDB code 4BCC); (D) compound **9i** (PDB code 4BCD). PREP and inhibitor carbon atoms are colored gray and green, respectively. Hydrogen bonds are drawn as thin lines. The σ_A weighted $2mF_o - \Delta F_c$ electron density using phases from the final model is contoured at the 1σ level, where σ represents the rms electron density for the unit cell. Contours more than 1.4 Å from any of the displayed atoms have been removed for clarity. The figure was drawn using Molscript[31] and rendered with Raster 3D.[32]

and **9i** (Figure 3) closely resembles that of the Z-Pro-prolinal (ZPP) complex determined previously.[24a]

The P1 pyrrolidine ring occupies the snug P1 pocket, and additional specificity is provided by a ring stacking interaction with Trp595. The carbonitrile of compounds **13** and **14**, equivalent to the aldehyde group of ZPP, is stabilized by hydrogen bonds with the main chain NH of Asn555 that follows the catalytic Ser (as observed with all α/β-hydrolase enzymes) and with the phenolic OH of Tyr473.[33] Hydrogen bonds are made between the inhibitor P2 carbonyl and the

dx.doi.org/10.1021/jm301060g | *J. Med. Chem.* 2012, 55, 9856−9867

guanidino group of Arg643 and between the P3 carbonyl and the side chain NH of Trp595 (Figure 3B,C). The consistent increase in inhibitor potency when changing a P3-Z function for a 4-phenylbutanoyl residue (for example, **9f** vs **9e**, and **9h** vs **9g**) can be understood when comparing the crystal structure of PREP in complex with ZPP with the structures for complexes with the novel compounds. The longer phenylbutanoyl substituent is bound snugly into this P3 pocket, while the Z group that is two carbons shorter would not fit this pocket as efficiently, resulting in the diminished inhibitory activity.

In the complex containing compound **13**, there is clear electron density for the azide group of the P2 substituent (Figure 3B), and there is a hydrogen bond between the terminal nitrogen of this group and the phenolic OH of Tyr473 that also stabilizes the oxyanion during substrate hydrolysis. The IC_{50} of this inhibitor (0.003 μM) is characterized by a 2-fold increase in potency over the equivalent compound **17** that has a hydrogen atom at this position (IC_{50} = 0.006 μM) and by a 3-fold increase over compound **14** (IC_{50} = 0.009 μM). While no additional direct interactions are made with compound **14**, the *tert*-butyl group of this inhibitor lies only 3.8 Å away from the OH group of Tyr471. This suggests that incorporating some additional polar functionality in this part of the inhibitor could yield enhanced binding. Also, the carbonyl part of the Boc group is bound to a solvent glycerol molecule, suggesting that expansion of this part of compound **14** could displace this glycerol for further enhanced binding (Figure 3C).

Unlike the Boc-protected aminomethyl substituent of compound **14** that binds close to the edge of the enzyme cavity, the 4-fluorophenyl substituent of compound **9i** points into the center of the enzyme cavity (Figure 3D). Despite the differences in binding mode of these substituents, the very similar IC_{50} values for compounds **9f** and **9i** suggest that this differential binding does not have a large effect on potency. In addition, the binding mode determined for **9i** cannot explain the increased PREP affinity when compared to its non-fluorinated analogue **9h**, as neither the fluorine atom nor the phenyl ring is engaged in specific interactions with the enzyme.

Nonetheless, it is clear from these results that the inhibitors' P2 substituents that are the subject of this report can in general be expected to be accommodated in a region of PREP that hitherto has not been probed by inhibitors (Figure 4). With regard to the three complexed inhibitors, only the P2-azido substituent in **13** was found to provide additional enthalpic stabilization of the crystallized enzyme−inhibitor complex. However, the potential involvement of stabilizing interactions mediated by other P2 substituents in compounds **9a**−**v** cannot be excluded. In a more general view, further compound optimization by applying the insights provided by this crystallographic study (as exemplified for compound **14**) seems a realistic goal. Finally, it is worth mentioning that the dimensions of the P2-substituent-accommodating cavity are large enough to allow for very bulky substituent moieties. These could include fluorophores, liganded metal ions, and related functionalities that typically serve as reporter groups, for example, in activity-based probes for proteases.[35]

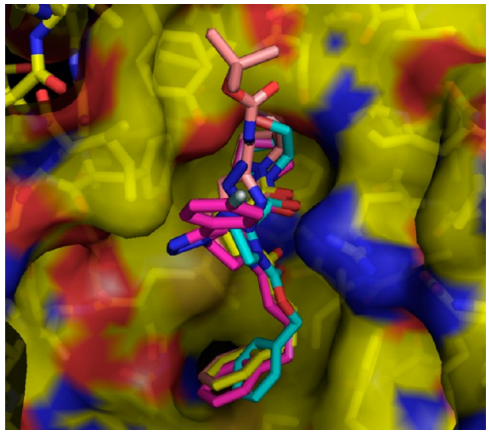

Figure 4. Electrostatic surface of prolyl oligopeptidase−inhibitor complexes. Carbon atoms are colored cyan for ZPP, yellow for compound **13**, salmon for compound **14**, and magenta for compound **9i**. The figure was drawn with PyMOL.[34]

High-Content Analysis of the Effect of PREP Inhibitors on α-Synuclein Aggregation and Apoptosis in a Cellular Synucleinopathy Model. α-Synuclein (α-SYN) is mainly a neuronal protein, accounting in nonpathological conditions for up to 1% of the protein content in the cytosol. The functional characterization of the protein is hitherto far from complete: several hypotheses are currently investigated, but there is mounting evidence that α-SYN is functioning as a chaperone in the formation of SNARE complexes and in this way is involved in vesicular trafficking and the cellular functioning of the neural Golgi apparatus. The soluble form of α-SYN can aggregate into insoluble fibrils in pathological conditions characterized by intracellular Lewy bodies, such as Parkinson's disease, Lewy body dementia, and multiple system atrophy.[36] Recently, PREP was reported to accelerate the aggregation of α-SYN and the formation of fibrils in a cell-free in vitro model.[20,37] Moreover, small-molecule inhibitors of PREP were demonstrated to reverse the aggregation process in the same model. Very recently, reference **17** was reported to also reduce α-SYN aggregation in cellulo and in vivo.[38] These findings, together with literature evidence for the interaction between α-SYN and PREP in cells with high expression of α-SYN, led us to evaluate a number of our PREP inhibitors in a model of synucleinopathy in SH-SY5Y5 human neuroblastoma cells that overexpress α-SYN.[39] Compounds **9f**, **9i**, **13**, **14** were selected. These molecules are among the most potent and selective novel inhibitors we identified during this study.

Prior to the start of the aggregation experiments, cellular permeation potential was determined. By reliance on a standard protocol, the SH-SY5Y5 cells were incubated with different concentrations of compounds **9i**, **9f**, **13**, **14**, and **16** for 24 h. The supernatant was subsequently washed away, and remaining PREP activity in the cells was evaluated after lysis, using a standard colorigenic activity assay (Figure 5). The data obtained indicate optimal but still moderate membrane permeability for compounds **13** and **14**. The latter inhibitors were therefore forwarded to the aggregation experiments. Reference **16** was not able to significantly reduce intracellular PREP activity under these conditions (data not shown) and was omitted in the cellular α-Syn aggregation experiments.

In the α-SYN aggregation experiments, the SH-SY5Y neuroblastoma cells overexpressing α-SYN were exposed to oxidative stress conditions using H_2O_2 and $FeCl_2$. As described earlier, these conditions led to the formation of α-SYN aggregates, detected by thioflavin S staining, and to apoptosis, measured as nuclear condensation and fragmentation. Both parameters (aggregate formation and nucleus condensation/fragmentation) were used as end points to evaluate the effect of PREP inhibitors. After fixation, the cells were analyzed with an

dx.doi.org/10.1021/jm301060g | J. Med. Chem. 2012, 55, 9856−9867

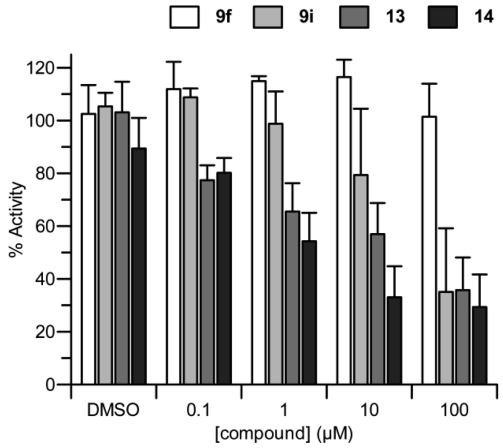

Figure 5. Membrane permeability of inhibitors **9f**, **9i**, **13**, and **14** determined by measuring residual PREP activity in SH-SY5Y cells after incubation with different inhibitor concentrations for 24 h, followed by washing away of the supernatant and lysis of the cells. Residual activity is defined as the % of PREP activity relative to untreated cells that remains after incubation and washing, measured using the colorigenic substrate Z-Gly-Pro-*p*-nitroanilide.

automated image acquisition and analysis protocol. To facilitate the quantitative analysis of α-SYN inclusion formation in this cell culture model, a high-content multiparametric method was used.[38]

Next, the concentration dependence of the effect on α-SYN aggregation was investigated for the two most active compounds, **13** and **14**. The corresponding data, summarized in Figure 6, suggest EC_{50} values in the low micromolar region for the molecules. The observation that compound **13** consistently displays a somewhat lower effective concentration than **14** is in line with the measured difference in IC_{50} for both as inhibitors of PREP. Altogether, the cell permeability, the low micromolar EC_{50} values, and the maximal reduction in cell numbers displaying α-SYN aggregation are equivalent to the results obtained earlier for compound **17** in this model.[38] The maximal reduction in α-SYN aggregation is also comparable to that induced by tacrolimus, the most potent compound identified so far in this model.[39] The latter, however, has an EC_{50} in the low nanomolar range. Taking into account the moderate cell permeability of the compounds (Figure 5), these data indicate that the intrinsic potential of PREP inhibitors to reduce α-SYN aggregate formation in this model is considerable.

Both **13** and **14** also significantly reduced the number of cells in late apoptosis. Although apoptosis in this model has been shown to be positively correlated to occurrence of α-SYN aggregates, several other, yet unidentified factors appear to be influencing the apoptotic processes as well.[39] Therefore, care should be taken in interpreting this end point and in comparing it to the effect on α-SYN aggregation. Nonetheless, since synucleinopathies are characterized by important neuronal apoptotic processes, we decided to include this parameter in our analysis as an additional criterion to select compounds for potential evaluation in more advanced preclinical models of synucleinopathy. Again, the maximal effect on apoptosis of **13** and **14** is roughly comparable to what has been reported earlier for tacrolimus and **17** in this model.

CONCLUSION

We have investigated the effect on affinity of regioselectively introduced substituents in the S2-binding part of the typical dipeptide-derived basic structure of PREP inhibitors. Such modifications could be used to modify or tune the target affinity, the selectivity, and the physicochemical parameters in drug discovery programs focusing on PREP inhibitors. Biochemical evaluation of the produced inhibitors identified several substituent types that are able to significantly increase target affinity, thereby reducing the need for an electrophilic "warhead" functionality. Pronounced PREP specificity within the group of Clan SC proteases was generally observed for the novel molecules, comparable to the profile of several dipeptide-derived molecules that were reported earlier. Nonetheless, the presence of the additional substituent could also be expected to increase PREP selectivity with respect to other potential targets recognizing the dipeptidic architecture of PREP inhibitors or delay metabolization by dipeptide-processing enzymes. Furthermore, the structures of several inhibitor−PREP complexes were determined by X-ray crystallography. Finally, we studied selected compounds in a cellular model of synucleinopathy. Our results demonstrate that PREP inhibitors exert a significant antiaggregation potential on α-synuclein in SH-SY5Y cells, an effect that had been reported earlier in the same model for reference compound **17**. The experiments also suggest that the compounds influence late apoptosis in these cells. In conclusion, the obtained data call for extended investigation of these novel, selective, and high affinity PREP inhibitors in

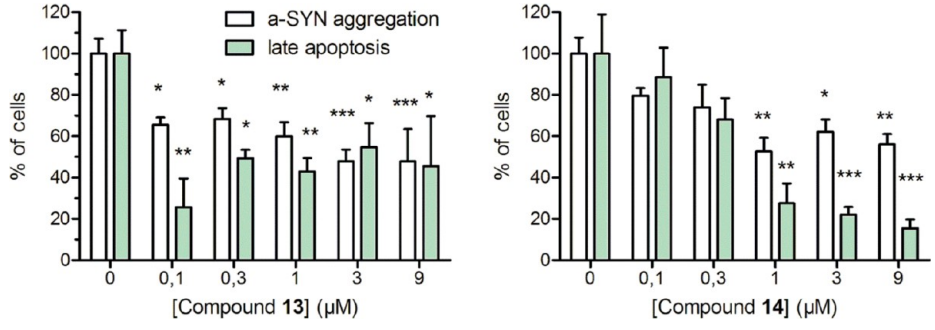

Figure 6. Effect of PREP inhibitors **13** and **14** on α-SYN aggregation and late apoptosis. SH-SY5Y cells were incubated with the inhibitors for 3 days under oxidative stress and then analyzed as described. The percentages of cells with α-SYN aggregates and of cells in late apoptosis are expressed as percentages of the number of cells recorded under control conditions (1% DMSO). Statistical significance compared to control (1% DMSO) was determined using ANOVA, followed by Dunnett's post-test with a significance level of 5%. This is represented as follows: (*) $p < 0.05$; (**) $p < 0.01$; (***) $p < 0.001$.

dx.doi.org/10.1021/jm301060g | J. Med. Chem. 2012, 55, 9856−9867

both in vitro and in vivo models of synucleinopathy. Such experiments could be instrumental to validate PREP as a druggable target for this class of diseases.[40] Additional effort to apply the design principles presented in this publication for obtaining PREP inhibitors with optimized cell permeability would, however, be desirable.

EXPERIMENTAL SECTION

Amino acids and TBTU were purchased from Novabiochem. Other reagents were obtained from Sigma-Aldrich or Acros and used as such unless otherwise specified. Characterization of intermediates and final compounds was done using NMR spectroscopy and mass spectrometry. Final purity was determined using HPLC analysis. ^{1}H NMR (400 MHz) and ^{13}C NMR (100 MHz) spectra were recorded on a Bruker Advance III Ultrashield 400 spectrometer. $CDCl_3$, CD_3OD, or DMSO-d_6 were used as the solvents. Chemical shifts in the spectra are given in ppm and coupling constants (J) in Hz. ES mass spectra were obtained with an Esquire 3000Plus ion trap mass spectrometer from Bruker Daltonics, using the direct infusion mode.

Purity of final products was determined using HPLC analysis. (1) LC/MS chromatograms were recorded on an Agilent 1100 series HPLC system equipped with an Alltech Prevail C18 column (2.1 mm × 50 mm × 3 μm) connected to an Esquire 3000Plus ion trap mass spectrometer from Bruker Daltonics. A 5−100% acetonitrile/water, 20 min gradient, was used with a flow rate of 0.2 mL/min. Formic acid (0.1%) was added to both solvents. (2) In addition, reversed phase HPLC chromatograms were recorded on a Gilson instrument equipped with an Ultra Sphere ODS column (4.6 mm × 250 mm × 5 μm) and a UV detector. A 10−100% acetonitrile, 35 min gradient, was used with a flow rate of 1 mL/min. Then 0.1% trifluoroacetic acid was added to both solvents. An indicated purity of 100% indicates that no other peaks in the chromatogram occur. All final products reported in this publication were determined to have purities of ≥95%.

General Experimental and Analytical Data for Key Products 9c, 9i, 9r, and 14. Detailed experimental and analytical data for all intermediates and final products in the manuscript can be found in the Supporting Information.

1-((2*S*,4*S*)-4-(4-Cyclopropyl-1*H*-1,2,3-triazol-1-yl)-2-(pyrrolidine-1-carbonyl)pyrrolidin-1-yl)-4-phenylbutan-1-one (9c). Azide **7b** (0.28 mmol, 100 mg, 1 equiv) was dissolved in methanol. To this solution was added ethynylcyclopropane (0.34 mmol, 23 mg, 1.2 equiv), followed by CuI (0.028 mmol, 5.3 mg, 0.1 equiv) and Et_3N (trace). The reaction mixture was stirred for 24 h at room temperature, after which thin-layer chromatography was used to demonstrate complete consumption of the starting material. The volatile components were then evaporated, and the target compound was isolated after flash chromatography (hexanes to hexanes/ethyl actetate, 1:1), mainly for removing copper residues. The target compound was obtained as a colorless oil that transformed upon standing into an amorphous solid. ^{1}H NMR ($CDCl_3$, 400 MHz): δ 0.97 (m, 2H, CH_2); 1.42 (m, 2H, CH_2); 1.76−2.12 (m, 6H, CH_2); 2.24−2.39 (m, 3H, CH_2 + CH); 2.67 (t, J = 7.2 Hz, 2H, CH_2); 2.79−2.93 (m, 1H, CH_2); 3.18−3.30 (m, 1H, CH_2); 3.36−3.45 (m, 2H, CH_2); 3.54−3.68 (m, 1H, CH_2); 3.82 (t, 1H, J = 9.6 Hz, CH_2); 3.94 (q, J = 8 Hz, 1H, CH_2); 4.13 (t, J = 9.6 Hz, 1H, CH_2); 4.8 (t, J = 8 Hz, 1H, CH_2); 5.29 (quin, J = 8 Hz, 1H, CH_2); 7.14−7.21 (m, 3H, CH_{ar}); 7.24−7.31 (m, 2H, CH_{ar}); 7.71 (s, 1H, CH_{ar}). ESI-MS$^+$: m/z = 422.3 $[M + H]^+$. Purity determination: (1) RP-HPLC, t_R = 18.44 min, purity = 97.31%; (2) LC/MS, t_R = 13.4 min, purity = 96%.

1-((2*S*,4*S*)-4-(4-(4-Fluorophenyl)-1*H*-1,2,3-triazol-1-yl)-2-(pyrrolidine-1-carbonyl)pyrrolidin-1-yl)-4-phenylbutan-1-one (9i). A procedure identical to the one used for the preparation of compound **9c** was applied using azide **7b** (0.28 mmol, 100 mg, 1 equiv), 1-ethynyl-4-fluorobenzene (0.34 mmol, 40 mg, 1.2 equiv), CuI (0.028 mmol, 5.3 mg, 0.1 equiv), and Et_3N (trace). After chromatography, the target product was obtained as a colorless oil that transformed upon standing into an amorphous solid. ^{1}H NMR ($CDCl_3$, 400 MHz): δ 1.82−2.12 (m, 6H, CH_2); 2.32 (t, J = 7.2 Hz, 2H, CH_2); 2.34−2.51 (m, 1H, CH_2); 2.68 (t, J = 7.6 Hz, 2H, CH_2); 2.9−3.01 (m, 1H, CH_2); 3.38−3.51 (m, 2H, CH_2); 3.56−3.67 (quin, J = 7.2 Hz, 1H, CH_2); 3.88−4.06 (m, 2H, CH_2); 4.2 (t, J = 7.6 Hz, 1H, CH_2); 4.85 (t, J = 7.6 Hz, 1H, CH_2); 5.43 (t, J = 7.6 Hz, 1H, CH_2); 7.12 (t, J = 8 Hz, 3H, CH_{ar}); 7.18 (d, J = 7.2 Hz, 2H, CH_{ar}); 7.26 (t, J = 8 Hz, 2H, CH_{ar}); 7.81 (dt, J = 8 Hz, J = 2 Hz, 2H, CH_{ar}); 8.24 (s, 1H, CH_{ar}). ESI-MS$^+$: m/z = 476.2 $[M + H]^+$. Purity determination: (1) RP-HPLC, t_R = 30.06 min, purity = 99%; (2) LC/MS, t_R = 16.2 min, purity = 98%.

1-((2*S*,4*S*)-4-(4-((Dimethylamino)methyl)-1*H*-1,2,3-triazol-1-yl)-2-(pyrrolidine-1-carbonyl)pyrrolidin-1-yl)-4-phenylbutan-1-one (9r). A procedure identical to the one used for the preparation of compound **9c** was applied using azide **7b** (0.28 mmol, 100 mg, 1 equiv), *N*,*N*-dimethylprop-2-yn-1-amine (0.34 mmol, 28 mg, 1.2 equiv), CuI (0.028 mmol, 5.3 mg, 0.1 equiv), and Et_3N (trace). After chromatography, the target product was obtained as a colorless oil that transformed upon standing into an amorphous solid. ^{1}H NMR ($CDCl_3$, 400 MHz): δ 1.81−2.14 (m, 6H, CH_2); 2.2−2.31 (m, 8H, CH_2, CH_3); 2.36−2.44 (m, 1H, CH_2); 2.67 (t, J = 7.6 Hz, 2H, CH_2); 2.81−2.92 (m, 1H, CH_2); 3.34−3.41 (m, 2H, CH_2); 3.48 (s, 2H, CH_2); 3.54−3.62 (m, 1H, CH_2); 3.86−3.97 (m, 2H, CH_2); 4.17 (t, J = 7.6 Hz, 1H, CH_2); 4.79 (t, J = 7.6 Hz, 1H, CH_2); 5.28 (quin, J = 7.6 Hz, 1H, CH); 7.16 (d, J = 7.6 Hz, 2H, CH_{ar}); 7.28 (t, J = 7.6 Hz, 3H, CH_{ar}); 7.91 (d, J = 7.6 Hz, 1H, CH_{ar}). ESI-MS$^+$: m/z = 439.6 $[M + H]^+$, 461.3 $[M + Na]^+$. Purity determination: (1) RP-HPLC, t_R = 13.98 min, purity = 100%; (2) LC/MS, t_R = 18.3 min, purity = 99%.

***tert*-Butyl ((1-((3*S*,5*S*)-5-((*S*)-2-Cyanopyrrolidine-1-carbonyl)-1-(4-phenylbutanoyl)pyrrolidin-3-yl)-1*H*-1,2,3-triazol-4-yl)methyl)carbamate (14).** A procedure identical to the one used for the preparation of compound **9c** was applied using azide **13** (0.26 mmol, 100 mg, 1 equiv), *N*-Boc-propargylamine (0.34 mmol, 50 mg, 1.2 equiv), CuI (0.026 mmol, 5.0 mg, 0.1 equiv), and Et_3N (trace) and using dichloromethane (5 mL) as the solvent instead of methanol. After chromatography, the target product was obtained as a colorless oil that transformed upon standing into an amorphous solid. ^{1}H NMR ($CDCl_3$, 400 MHz): δ 1.44 (s, 9H, CH_3); 1.92−2.06 (m, 3H, CH_2); 2.18−2.33 (m, 5H, CH_2); 2.39−2.5 (m, 1H, CH_2); 2.66 (quin, J = 8 Hz, 2H, CH_2); 2.84−2.95 (m, 1H, CH_2); 3.58−3.68 (m, 1H, CH); 3.88 (t, J = 8.2 Hz, 1H, CH_2); 3.91−3.98 (m, 1H, CH); 4.17 (t, J = 8.2 Hz, 1H, CH_2); 4.34−4.49 (m, 2H, CH_2); 4.7 (t, J = 8 Hz, 1H, CH); 4.79−4.86 (m, 1H, CH); 5.13 (br s, 1H, NH) 5.26 (t, J = 8 Hz, 1H, CH); 7.18 (t, J = 8 Hz, 3H, CH_{ar}); 7.26 (m, 2H, CH_{ar}); 7.76 (s, 1H, CH_{ar}). ESI-MS$^+$: m/z = 536.3 $[M + H]^+$. Purity determination: (1) RP-HPLC, t_R = 26.2 min, purity = 98.4%; (2) LC/MS, t_R = 18.3 min, purity = 98.8%.

ASSOCIATED CONTENT

Supporting Information

(1) General synthetic procedures, (2) compound characterization data, (3) enzymatic assay conditions, (4) crystallographic data, and (5) the SH-SY5Y cellular assay conditions. This material is available free of charge via the Internet at http://pubs.acs.org.

AUTHOR INFORMATION

Corresponding Author

*Phone: +32-3-2652708. E-mail: pieter.vanderveken@ua.ac.be.

Notes

The authors declare no competing financial interest.

ACKNOWLEDGMENTS

This work received support from the EU FP7-HEALTH-2007-B, proposal No. 223077 (nEuroPro), the Flanders Research Foundation (FWO, Project G.0114.08), BOF GOA (Research Council of University of Antwerp, Belgium), and the Hercules Foundation. Crystallographic data were collected at beamline IO4 at Diamond Light Source, U.K., and we acknowledge the support of Ralf Flaig. Nicole Lamoen and Sophie Lyssens are

thanked for their excellent technical assistance. The Laboratory of Medicinal Chemistry and Laboratory of Medical Biochemistry, University of Antwerp, are partners of the Antwerp Drug Discovery Network (ADDN).

■ ABBREVIATIONS USED

DPP, dipeptidyl peptidase; FAP, fibroblast activation protein; POP, prolyl oligopeptidase; PO, prolyl oligopeptidase; PREP, prolyl oligopeptidase; SNARE, soluble NSF attachment receptor protein; α-SYN, α-synuclein; ZPP, *N*-benzyloxycarbonylprolylprolinal

■ ADDITIONAL NOTE

Prolyl oligopeptidase, formerly known as prolyl endopeptidase, has received several abbreviations (PREP, PEP, POP, PO). In this paper we refer to it as PREP, which relates to the unique name of the *PREP* gene as found in gene and protein databases.

■ REFERENCES

(1) Walter, R. Partial purification and characterization of post-proline cleaving enzyme: enzymatic inactivation of neurohypophyseal hormones by kidney preparations of various species. *Biochim. Biophys. Acta* **1976**, *422* (1), 138−158.

(2) Garcia-Horsman, J. A.; Mannisto, P. T.; Venalainen, J. I. On the role of prolyl oligopeptidase in health and disease. *Neuropeptides* **2007**, *41* (1), 1−24.

(3) Brandt, I.; Scharpe, S.; Lambeir, A. M. Suggested functions for prolyl oligopeptidase: a puzzling paradox. *Clin. Chim. Acta* **2007**, *377* (1−2), 50−61.

(4) Umemura, K.; Kondo, K.; Ikeda, Y.; Kobayashi, T.; Urata, Y.; Nakashima, M. Pharmacokinetics and safety of JTP-4819, a novel specific orally active prolyl endopeptidase inhibitor, in healthy male volunteers. *Br. J. Clin. Pharmacol.* **1997**, *43* (6), 613−618.

(5) Morain, P.; Robin, J. L.; De Nanteuil, G.; Jochemsen, R.; Heidet, V.; Guez, D. Pharmacodynamic and pharmacokinetic profile of S 17092, a new orally active prolyl endopeptidase inhibitor, in elderly healthy volunteers. A phase I study. *Br. J. Clin. Pharmacol.* **2000**, *50* (4), 350−359.

(6) Morain, P.; Lestage, P.; De Nanteuil, G.; Jochemsen, R.; Robin, J. L.; Guez, D.; Boyer, P. A. S 17092: a prolyl endopeptidase inhibitor as a potential therapeutic drug for memory impairment. Preclinical and clinical studies. *CNS Drug. Rev.* **2002**, *8* (1), 31−52.

(7) Bellemere, G.; Morain, P.; Vaudry, H.; Jegou, S. Effect of S 17092, a novel prolyl endopeptidase inhibitor, on substance P and alpha-melanocyte-stimulating hormone breakdown in the rat brain. *J. Neurochem.* **2003**, *84* (5), 919−929.

(8) Jalkanen, A. J.; Puttonen, K. A.; Venalainen, J. I.; Sinerva, V.; Mannila, A.; Ruotsalainen, S.; Jarho, E. M.; Wallen, E. A.; Mannisto, P. T. Beneficial effect of prolyl oligopeptidase inhibition on spatial memory in young but not in old scopolamine-treated rats. *Basic Clin. Pharmacol. Toxicol.* **2007**, *100*, 132−138.

(9) Williams, R. S.; Eames, M.; Ryves, W. J.; Viggars, J.; Harwood, A. J. Loss of a prolyl oligopeptidase confers resistance to lithium by elevation of inositol (1,4,5) trisphosphate. *EMBO J.* **1999**, *18* (10), 2734−2745.

(10) Williams, R. S.; Cheng, L.; Mudge, A. W.; Harwood, A. J. A common mechanism of action for three mood-stabilizing drugs. *Nature* **2002**, *417* (6886), 292−295.

(11) (a) Di Daniel, E.; Glover, C. P.; Grot, E.; Chan, M. K.; Sanderson, T. H.; White, J. H.; Ellis, C. L.; Gallagher, K. T.; Uney, J.; Thomas, J.; Maycox, P. R.; Mudge, A. W. Prolyl oligopeptidase binds to GAP-43 and functions without its peptidase activity. *Mol. Cell. Neurosci.* **2009**, *41* (3), 373−382. (b) Szeltner, Z.; Morawski, M.; Juhasz, T.; Szamosi, I.; Liliom, K.; Csizmok, V.; Tolgyesi, F.; Polgar, L. GAP43 shows partial co-localisation but no strong physical interaction with prolyl oligopeptidase. *Biochim. Biophys. Acta* **2010**, *1804*, 2162−76.

(12) Warden, C. H.; Fisler, J. S.; Espinal, G.; Graham, J.; Havel, P. J.; Perroud, B. Maternal influence of prolyl endopeptidase on fat mass of adult progeny. *Int. J. Obes.* **2009**, *33* (9), 1013−1016.

(13) Perroud, B.; Alvarado, R. J.; Espinal, G. M.; Morado, A. R.; Phinney, B. S.; Warden, C. H. In vivo multiplex quantitative analysis of 3 forms of alpha melanocyte stimulating hormone in pituitary of prolyl endopeptidase deficient mice. *Mol. Brain* **2009**, *2* (1), 14.

(14) Schulz, I.; Gerhartz, B.; Neubauer, A.; Holloschi, A.; Heiser, U.; Hafner, M.; Demuth, H. U. Modulation of inositol 1,4,5-triphosphate concentration by prolyl endopeptidase inhibition. *Eur. J. Biochem.* **2002**, *269* (23), 5813−5820.

(15) Schulz, I.; Zeitschel, U.; Rudolph, T.; Ruiz-Carrillo, D.; Rahfeld, J. U.; Gerhartz, B.; Bigl, V.; Demuth, H. U.; Rossner, S. Subcellular localization suggests novel functions for prolyl endopeptidase in protein secretion. *J. Neurochem.* **2005**, *94* (4), 970−979.

(16) Rossner, S.; Schulz, I.; Zeitschel, U.; Schliebs, R.; Bigl, V.; Demuth, H. U. Brain prolyl endopeptidase expression in aging, APP transgenic mice and Alzheimer's disease. *Neurochem. Res.* **2005**, *30* (6−7), 695−702.

(17) Moreno-Baylach, M. J.; Felipo, V.; Mannisto, P. T.; Garcia-Horsman, J. A. Expression and traffic of cellular prolyl oligopeptidase are regulated during cerebellar granule cell differentiation, maturation, and aging. *Neuroscience* **2008**, *156* (3), 580−585.

(18) Agirregoitia, N.; Bizet, P.; Agirregoitia, E.; Boutelet, I.; Peralta, L.; Vaudry, H.; Jegou, S. Prolyl endopeptidase mRNA expression in the central nervous system during rat development. *J. Chem. Neuroanat.* **2010**, *40* (1), 53−62.

(19) Myohanen, T. T.; Garcia-Horsman, J. A.; Tenorio-Laranga, J.; Mannisto, P. T. Issues about the physiological functions of prolyl oligopeptidase based on its discordant spatial association with substrates and inconsistencies among mRNA, protein levels, and enzymatic activity. *J. Histochem. Cytochem.* **2009**, *57* (9), 831−848.

(20) Brandt, I.; Gerard, M.; Sergeant, K.; Devreese, B.; Baekelandt, V.; Augustyns, K.; Scharpe, S.; Engelborghs, Y.; Lambeir, A. M. Prolyl oligopeptidase stimulates the aggregation of alpha-synuclein. *Peptides* **2008**, *29* (9), 1472−1478.

(21) Lawandi, J.; Gerber-Lemaire, S.; Juillerat-Jeanneret, L.; Moitessier, N. Inhibitors of prolyl oligopeptidases for the therapy of human diseases: defining diseases and inhibitors. *J. Med. Chem.* **2010**, *53* (9), 3423−3438.

(22) (a) Z-Pro-prolinal was originally described in the following: Friedman, T. C.; Orlowski, M.; Wilk, S. Prolyl endopeptidase: inhibition in vivo by *N*-benzyloxycarbonyl-prolyl-prolinal. *J. Neurochem.* **1984**, *42* (1), 237−241. (b) JTP-4819 was originally reported in the following: Wallen, E. A. A.; Christiaans, J. A. M.; Saario, S. M.; Forsberg, M. M.; Venalainen, J. I.; Paso, H. M.; Mannisto, P. T.; Gynther, J. 4-Phenylbutanoyl 2(*S*)-acylpyrrolidines and 4-phenylbutanoyl-L-prolyl-2(*S*)-acylpyrrolidines as prolyl oligopeptidase inhibitors. *Bioorg. Med. Chem.* **2002**, *10* (7), 2199−2206. (c) Compound **3** was reported in the following: Haffner, C. D.; Diaz, C. J.; Miller, A. B.; Reid, R. A.; Madauss, K. P.; Hassel, A.; Hanlon, M. H.; Porter, D. J. T.; Becherer, J. D.; Carter, L. H. *Bioorg. Med. Chem. Lett.* **2008**, *18*, 4360−4363. (d) Compound **4** was reported in the following: Tran, T.; Quan, C.; Edosada, C. Y.; Mayeda, M.; Wiesmann, C.; Sutherlin, D.; Wolf, B. B. Synthesis and structure−activity-relationship of *N*-acyl-Gly, *N*-acyl-Sar and *N*-blocked boroPro inhibitors of FAP, DPP IV and POP. *Bioorg. Med. Chem. Lett.* **2007**, *17* (5), 1438−1442.

(23) Van der Veken, P.; Haemers, A.; Augustyns, K. Prolyl peptidases related to dipeptidyl peptidase IV: potential of specific inhibitors in drug discovery. *Curr. Top. Med. Chem* **2007**, *7* (6), 621−635.

(24) (a) Fulop, V.; Szeltner, Z.; Renner, V.; Polgar, L. Structures of prolyl oligopeptidase substrate/inhibitor complexes. Use of inhibitor binding for titration of the catalytic histidine residue. *J. Biol. Chem.* **2001**, *276* (2), 1262−1266 (corresponding PDB entry, 1E8N). (b) Fulop, V.; Bocskei, Z.; Polgar, L. Prolyl oligopeptidase: an unusual beta-propeller domain regulates proteolysis. *Cell* **1998**, *94* (2), 161−170 (corresponding PDB entry, 1QFS). (c) Kanai, K.; Aranyi, P.; Bocskei, Z.; Ferenczy, G.; Harmat, V.; Simon, K.; Batori, S.; Naray-Szabo, G.; Hermecz, I. Prolyl oligopeptidase inhibition by *N*-acyl-Pro-

pyrrolidine-type molecules. *J. Med. Chem.* **2008**, *51*, 7514−7522 (corresponding PDB entries, 3EQ7 and 3EQ8). (d) Reference 22c (corresponding PDB entry, 3DDU).

(25) (a) Venalainen, J. I.; Garcia-Horsman, J. A.; Forsberg, M. M.; Jalkanen, A.; Wallen, E. A. A.; Jarho, E. M.; Christiaans, J. A. M.; Gynther, J.; Mannisto, P. T. Binding kinetics and duration of in vivo action of prolyl oligopeptidase inhibitors. *Biochem. Pharmacol.* **2006**, *71* (5), 683−692. (b) Zhai, W.; Cardell, M.; De Meester, I.; Augustyns, K.; Hillinger, S.; Inci, I.; Arni, S.; Jungraithmayr, W.; Scharpé, S.; Weder, W.; Korom, S. Ischemia/reperfusion injury: the role of CD26/dipeptidyl-peptidase IV inhibition in lung transplantation. *Transplant. Proc.* **2006**, *38* (10), 3369−3371.

(26) (a) Webb, T. R.; Eigenbrot, C. Conformationally restricted arginine analogs. *J. Org. Chem.* **1991**, *56*, 3009−3016. (b) in Haitao, J.; Gomez-Vidal, J. A.; Martasek, P.; Roman, L.; Silverman, R. B. Conformationally restricted dipeptide amides as potent and selective neuronal nitric oxide synthase inhibitors. *J. Med. Chem.* **2006**, *49*, 6253−6264.

(27) Rostovstsev, V. V.; Green, L. G.; Fokin, V. F.; Sharpless, K. B. A stepwise Huisgen cycloaddition process: Cu-I-catalyzed regioselective ligation of azides and terminal alkynes. *Angew. Chem., Int. Ed.* **2002**, *41* (14), 2596−2599.

(28) (a) Van der Veken, P.; De Meester, I.; Dubois, V.; Soroka, A.; Van Goethem, S.; Maes, M. B.; Brandt, I.; Lambeir, A. M.; Chen, X.; Haemers, A.; Scharpe, S.; Augustyns, K. Inhibitors of dipeptidyl peptidase 8 and dipeptidyl peptidase 9. Part 1: Identification of dipeptide derived leads. *Bioorg. Med. Chem. Lett.* **2008**, *18* (14), 4154−8. (b) Van Goethem, S.; Van der Veken, P.; Dubois, V.; Soroka, A.; Lambeir, A. M.; Chen, X.; Haemers, A.; Scharpe, S.; De Meester, I.; Augustyns, K. Inhibitors of dipeptidyl peptidase 8 and dipeptidyl peptidase 9. Part 2: Isoindoline containing inhibitors. *Bioorg. Med. Chem. Lett.* **2008**, *18*, 4159−4162. (c) Van der Veken, P.; Soroka, A.; Brandt, I.; Chen, Y. S.; Maes, M. B.; Lambeir, A. M.; Chen, X.; Haemers, A.; Scharpe, S.; Augustyns, K.; De Meester, I. Irreversible inhibition of dipeptidyl peptidase 8 by dipeptide-derived diaryl phosphonates. *J. Med. Chem.* **2007**, *50*, 5568−5570. (d) Van Goethem, S.; Matheeussen, V.; Joossens, J.; Lambeir, A. M.; Chen, X.; De Meester, I.; Haemers, A.; Augustyns, K.; Van der Veken, P. Structure−activity relationship studies on isoindoline inhibitors of dipeptidyl peptidases 8 and 8 (DPP8, DPP9): Is DPP8-selectivity attainable? *J. Med. Chem.* **2011**, *54*, 5737−5746.

(29) (a) Yoshimoto, T.; Tsuru, D.; Yamamoto, N.; Ikezawa, R.; Furukawa, S. *Agric. Biol. Chem.* **1991**, *55* (1), 37−41. (b) Atack, J. R.; Suman-Chauhan, N.; Dawson, G.; Kulagowski, J. J. In vitro and in vivo inhibition of prolyl endopeptidase. *Eur. J. Pharmacol.* **1991**, *205* (2), 157−163.

(30) Jarho, E. M.; Venailainen, E. I.; Huuskonen, J.; Christiaans, J. A. M.; Forsberg, M. M.; Jairvinen, T.; Gynther, T.; Mannisto, P. T.; Wallèn, E.A.A. A cyclopent-2-enecarbonyl group mimics proline at the P2 position of prolyl oligopeptidase inhibitors. *J. Med. Chem.* **2004**, *47* (23), 5605−5607.

(31) Kraulis, P. J. MolScript: a program to produce both detailed and schematic plots of protein structures. *J. Appl. Crystallogr.* **1991**, *24*, 946−950.

(32) Merritt, E. A.; Murphy, M. E. P. Raster3D version 2.0. A program for photorealistic molecular graphics. *Acta Crystallogr. D* **1994**, *50*, 869−873.

(33) DeLano, W. L. *The PyMOL User's Manual*; DeLano Scientific, LLC: Palo Alto, CA, 2002.

(34) (a) Szeltner, Z.; Rea, D.; Renner, V.; Juliano, L.; Fülöp, V.; Polgár, L. Electrostatic environment at the active site of prolyl oligopeptidase is highly influential during substrate binding. *J. Biol. Chem.* **2003**, *278*, 48786−48793. (b) Rea, D.; Fülöp, V. Prolyl oligopeptidase structure and dynamics. *CNS Neurol. Disord.: Drug Targets* **2011**, *10*, 306−310.

(35) Sabido, E.; Tarrago, T.; Niessen, S.; Cravatt, B. F.; Giralt, E. Activity-based probes for measuring postproline protease activity. *ChemBioChem* **2009**, *10*, 2361−2366.

(36) Ostrerova-Golts, N.; Petrucelli, L.; Hardy, J.; Lee, J. M.; Farer, M.; Wolozin, B. The A53T alpha-synuclein mutation increases iron-dependent aggregation and toxicity. *J. Neurosci.* **2000**, *20*, 6048−6055.

(37) (a) Lambeir, A. M. Interaction of prolyl oligopeptidase with alpha-synuclein. *CNS Neurol. Disord.: Drug Targets* **2011**, *10*, 349−354. (b) Van Elzen, R.; Lambeir, A. M. Structure and function relationship in prolyl oligopeptidase. *CNS Neurol. Disord.: Drug Targets* **2011**, *10*, 297−305.

(38) Myöhänen, T. T.; Hannula, M. J.; Van Elzen, R.; Gerard, M.; Van Der Veken, P.; García-Horsman, J. A.; Baekelandt, V.; Männistö, P.; Lambeir, A. M. A prolyl oligopeptidase inhibitor, KYP-2047, reduces α-synuclein protein levels and aggregates in cellular and animal models of Parkinson's disease. *Br. J. Pharmacol.* **2012**, *166*, 1097−1113.

(39) Gerard, M.; Deleersnijder, A.; Daniels, V.; Schreurs, S.; Munck, S.; Reumers, V.; Pottel, H.; Engelborghs, Y.; Van den Haute, C.; Taymans, J. M.; Debyser, Z.; Baekelandt, V. Inhibition of FK506 binding proteins reduces alpha-synuclein aggregation and Parkinson's disease-like pathology. *J. Neurosci.* **2010**, *30*, 2454−2463.

(40) Lambeir, A. M. Translational research on prolyl oligopeptidase inhibitors: the long road ahead. *Expert Opin. Ther. Pat.* **2011**, *21*, 977−981.